

See discussions, stats, and author profiles for this publication at: <https://www.researchgate.net/publication/274095822>

Structural features of pyridylcinnamic acid dimers and their extended hydrogen-bonded aggregations

ARTICLE *in* JOURNAL OF MOLECULAR STRUCTURE · JUNE 2015

Impact Factor: 1.6 · DOI: 10.1016/j.molstruc.2014.11.041

READS

31

6 AUTHORS, INCLUDING:



Krisztián Csankó

University of Szeged

11 PUBLICATIONS 8 CITATIONS

SEE PROFILE



Pál Sipos

University of Szeged

101 PUBLICATIONS 1,106 CITATIONS

SEE PROFILE



Istvan Palinko

University of Szeged

233 PUBLICATIONS 1,750 CITATIONS

SEE PROFILE



Structural features of pyridylcinnamic acid dimers and their extended hydrogen-bonded aggregations

K. Csankó^{a,e}, K.I. Ruusuvaari^b, B. Tolnai^a, P. Sipos^{c,e}, O. Berkesi^{d,e}, I. Pálínkó^{a,e,*}

^a Department of Organic Chemistry, University of Szeged, Dóm tér 8, Szeged H-6720, Hungary

^b Department of Physics, Division of Atmospheric Sciences, University of Helsinki, Gustaf Hållströmin katu 2a, Helsinki FI-00560, Finland

^c Department of Inorganic and Analytical Chemistry, University of Szeged, Dóm tér 7, Szeged H-6720, Hungary

^d Department of Physical Chemistry and Material Sciences, University of Szeged, Aradi Vértanúk tere 1, Szeged H-6720, Hungary

^e Material and Solution Structure Research Group, Institute of Chemistry, University of Szeged, Szeged H-6720, Hungary

HIGHLIGHTS

- *E*-3-(*x*-pyridyl)propenoic acids (*x* = 2, 3 or 4) were synthesized.
- The structure forming abilities were investigated.
- Energies and bond lengths of C–H...N H-bonds were determined.
- Conformational behaviour of the acids and the zwitterionic forms were studied.

ARTICLE INFO

Article history:

Received 4 September 2014

Received in revised form 14 November 2014

Accepted 17 November 2014

Available online 23 November 2014

Keywords:

Pyridylpropenoic acids

Spectroscopic methods

Conformational search

Modelling intermolecular hydrogen bonds

ABSTRACT

The conformational as well as the structure-forming properties of *E*-3-(*x*-pyridyl)propenoic acids (*x* = 2, 3 or 4) have been studied with a combination of computational and spectroscopic methods. IR spectroscopy revealed that in the solid state the zwitterionic species predominate, while NMR measurements showed that dimers, kept together by strong C=O...H–O hydrogen bonds, were formed in a dipolar aprotic solvent (DMSO). In concentrated solution, extended aggregation occurred through the cooperative effect of (aromatic) C–H...N weak hydrogen bonds. Conformational search was performed at the HF/6-31G(d,p) level of theory. Comparison with experimental values as well as benchmarking calculations at several different levels of theory to probe the performance of the methods, B3LYP/6-31G++(d,p) method was found to be able to provide reasonable geometries as well as quantitative formation energies for the dimers and the tetramers, too.

© 2014 Elsevier B.V. All rights reserved.

Introduction

For some time, the family of cinnamic acid and its heteroatom-containing derivatives has been in the focus of our interest, due to their structural features allowing short- as well as long-range ordering in the liquid and the solid state as well [1–9]. They are also important pharmacologically, they act as enzyme inhibitors in cancer research [10], as new type of drugs against multiple resistant TBC bacteria [11], and as important intermediates in the chemical synthesis of pharmacologically active compounds [12,13].

In our previous studies, the combination of spectroscopic methods and molecular modelling was applied successfully for

the characterisation of the structure-forming interactions taking place in solution as well as in the solid state for furyl- [6] and thienyl-substituted cinnamic acids [9]. It was shown that the fundamental unit of the acids was the dimer, kept together by strong hydrogen bonds between the carboxylic groups, while the aggregation of the dimers occurred via weaker CH...X (X: O or S) interactions. Although these close contacts are weak, they are numerous, making the total interaction strong. Thus, they are crucial in keeping the molecular crystals together. Through applying computations, it was possible to pinpoint the most probable positions for the hydrogen bonds and to give reasonable estimates for their geometric parameters; however, energetic aspects were not touched. For the N-containing derivatives, only simple geometry optimizations were performed at the semiempirical level of theory [14–16] – assuming again that the dimer is the fundamental unit – since we were not successful in the syntheses of the molecules.

* Corresponding author at: Department of Organic Chemistry, University of Szeged, Dóm tér 8, Szeged H-6720, Hungary. Tel.: +36 62 544 288.

E-mail address: palinko@chem.u-szeged.hu (I. Pálínkó).

Since then, we have found ways for the preparation of some of the pyridyl-containing derivatives and now, the combined experimental and computational approach has become feasible. Results of this work is communicated in the followings.

Experimental

The molecules and their syntheses

Our choice for model compounds were the isomers of pyridyl-cinnamic acid: *E*-3'-(2-pyridyl)propenoic acid (**E2P**), *E*-3'-(3-pyridyl)propenoic acid (**E3P**), *E*-3'-(4-pyridyl)propenoic acid (**E4P**) and their sodium- and hydrochloride salts (Fig. 1). Although these molecules were rarely studied, simple NMR shift assignments and conformational analysis at low theoretical level have been done [17,18], and they were of help in checking the success of our synthetic work.

The model compounds were prepared by the Knoevenagel–Doebner condensation [19,20], taking place between the proper pyridine carboxaldehyde and malonic acid (Fig. 1) under basic conditions.

Details of the synthesis are as follows. Two equivalents of malonic acid were dissolved in four equivalents of pyridine at 50 °C; then, a catalytic amount of piperidine ($c_{\text{piperidine}} = 0.01 \text{ mol/L}$) was added to the reaction mixture. It was necessary to add traces of hydroquinone to the reaction at the beginning, to prevent radical polymerisation, probably taking place at higher temperatures. One equivalent of freshly distilled x -pyridinecarboxaldehyde ($x = 2, 3 \text{ or } 4$) was then added dropwise at 50 °C, under vigorous

stirring. After the addition of all components, the solution was stirred for an additional hour at 50 °C, to complete the condensation step; then, the mixture was heated to reflux for additional 5 h. It was needed for the complete decarboxylation of the intermediates, the 2-(x -pyridyl)methylenemalonic acids. The **E3P** and **E4P** compounds started to precipitate from the reaction mixture at the end of the first hour; however, the solution for the **E2P** synthesis, stayed clear over the time of the reaction.

Pyridine was removed from the reaction mixture on a rotary evaporator; then, the residue was diluted with cold diethyl ether, filtered, and washed twice with cold diethyl ether. The yield was 82–93%, and only the *E* isomer was formed. Due to the poor solubility of the compounds in any solvents except dipolar aprotic ones like DMSO (dimethyl sulfoxide) or DMF (N,N-dimethylformamide), they can be obtained with purity up to 99% without further purification. The sodium salts were prepared by the addition of one equivalent of NaOH in water, for each pyridylpropenoic acid. The hydrochloride salts were prepared with similar titration, i.e., with the addition of one equivalent of concentrated hydrochloric acid in water. The molecules prepared, are shown in Fig. 2.

Spectroscopic measurements

IR (infrared) measurements were carried out on a Bio-Rad FTS-40 FT-IR spectrometer, working in the reflection mode, using 1% of the sample in KBr (spectroscopic grade, Aldrich Chem. Co.) for the solid state and 0.1 mol/L solution in DMSO (Spectroscopic grade, Aldrich Chem. Co.) at 0.2 mm liquid thickness in quartz cuvette. 256 scans were collected for the spectra at 4 cm^{-1} resolution.

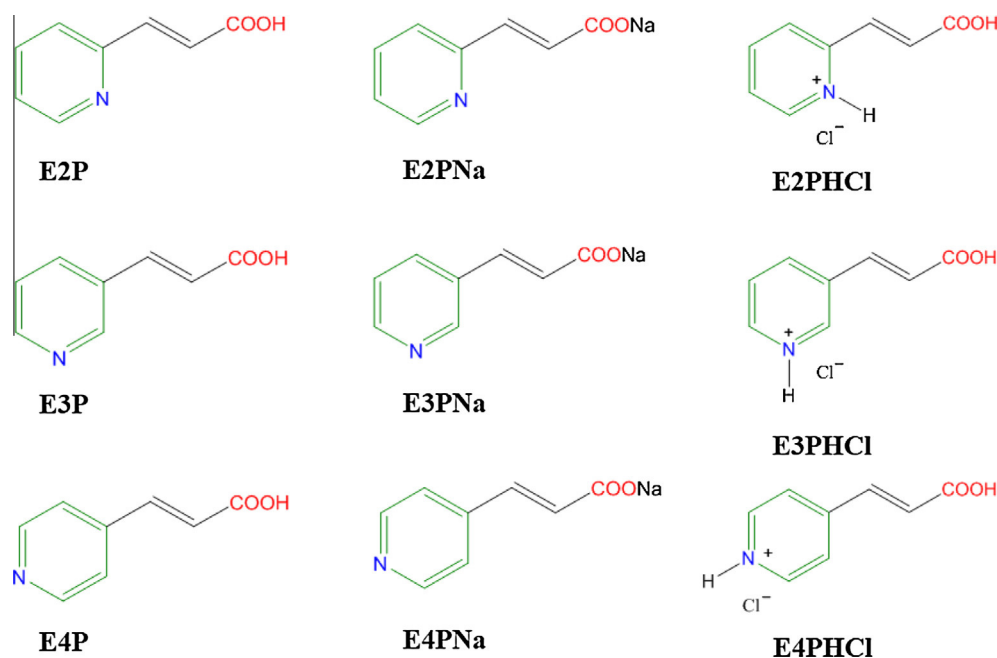


Fig. 1. The modified Knoevenagel–Doebner condensation.

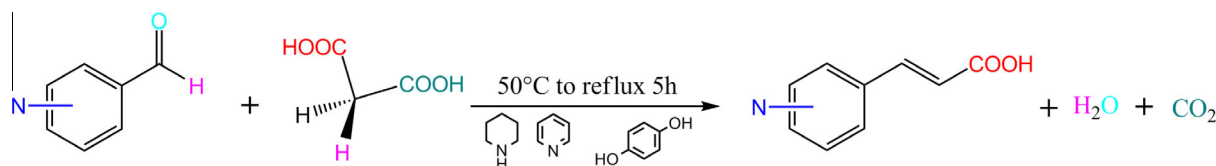


Fig. 2. The molecules studied.

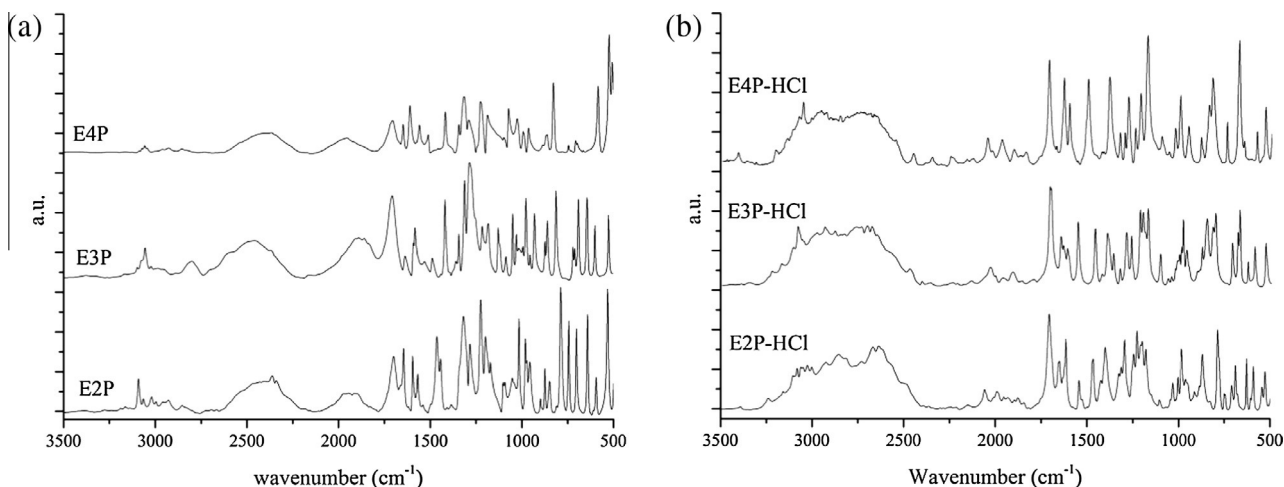


Fig. 3. Infrared spectra of the (a) zwitterions and the (b) hydrochloric salts in the solid state.

NMR measurements were performed in 0.5 mL DMSO- d_6 (99.96 atom% D, from Sigma–Aldrich Chem. Co.), using a Bruker Avance 500, 500 MHz NMR spectrometer with 5 mm glass NMR tubes from Wilmad. ^1H – ^1H correlation spectra were collected for the free acidic forms in saturated solution. The precise concentrations of the isomers were determined by gravimetry at room temperature (25 °C). They were as follows: 1.195 mol/L for **E2P**, 0.672 mol/L for **E3P** and 0.340 mol/L for **E4P**. 128 scans were collected for the proton spectra, and 16 scans at 1024×1024 resolution for the proton correlation spectra.

Computational methods

Calculations were performed for the **E2P** monomer and **E2P** dimer employing various *ab initio* and DFT methods (HF/6-31G(d,p), MP2/6-31G(d,p), B3LYP/6-31++G(d,p), B3LYP/CBSB7, B3LYPD3/6-31G(d,p), B3LYPD3/CBSB7, CBS-4M) using the Gaussian 2009 Rev. D.02 package [21]. In all energy calculations corrections for zero-point energy thermally corrected to 298 K (ZPE) and basis set superposition error (BSSE) have been performed. BSSE was taken into consideration through applying the Counterpoise (CP) method [22,23].

Initial guesses for the benchmark calculations were optimised with the semiempirical PM6 method; then, a conformational analysis was performed for the monomers, and the structure having the lowest energy was used as an initial guess. The actual benchmarking calculations consisted of geometry optimisations with energy calculations with the above-mentioned corrections and frequency calculations. Since we have access to limited computational resources, the main role of the benchmark calculations was to determine whether the HF/6-31G(d,p) method would perform adequately well and if not, which is the cheapest method, which gives satisfactory results already.

The benchmark results indicate that all methods resulted in planar geometries, for the individual molecules and for the hydrogen bonded dimers as well, except HF/6-31G(d,p), which performed well only for the individual monomers. Finally, it was decided to use the B3LYP/6-31++G(d,p) method for geometry optimisations and energy calculations for the larger hydrogen-bonded aggregates: this method produced reasonable estimates for the hydrogen bond energies as well as for geometric parameters. Our calculated hydrogen bond energy values were compared to that of the experimentally obtained -14.8 kcal/mol for the formic acid dimer [24]. Our calculated H...O distance and O–H...O values were compared to those of 163 pm and 171° , respectively, which

were the mean values derived from the crystal structures of 22 substituted or unsubstituted cinnamic acids [4]. Frequency calculations were performed to ensure that the stationary points were not transition states.

For the conformational search we used our own script to generate the input files. The sequence of the method was the following: after the determination of the two rotatable groups (the pyridyl and the carboxylic groups are the only rotatable parts in all three molecules), the software randomly generated 1024 variations for the two torsions of each individual monomer; then, the dihedral angles are frozen. The generated structures were optimised using the PM6 method, in order to test the generated structures, and to find faulty geometries. After the extraction of bad structures, the remaining ones were optimised and frequency checked at the HF/6-31G(d,p) level of theory (as it has already been mentioned, it worked well for the monomer), and the corrected energies were calculated, in order to find the lowest- and highest-energy structures; then, the energy surface was calculated to find the conformers belonging to the minima and to determine the rotational barriers separating the conformers. The sequence was done for each monomer of the acidic and the zwitterionic forms as well.

Results and discussion

Hydrogen-bonded interactions and conformational mobility by experiments

IR measurements revealed that the studied pyridylpropenoic acids were in the zwitterionic form in the solid state (Fig. 3a). The spectra lacked the wide absorption band around 3000 cm^{-1} , typical of hydrogen bonded acid dimers, but displayed a band at 2500 cm^{-1} , indicating the presence of a quaternary nitrogen.

The wide band in the $3200\text{--}2600\text{ cm}^{-1}$ range in the spectra of the hydrochloride salts indicated that dimerisation occurred via hydrogen bonds of the carboxylic groups, when the pyridyl nitrogen was protonated by a strong acid (Fig. 3b).

The IR study in solution with varying the concentration of pyridylcinnamic acids, could not be performed, because of the very limited solubility of the acids. They were only soluble in DMSO, and its IR absorptions overwhelmed the spectra suppressing bands of the acid, thus, making these measurements worthless. Therefore our attention was turned to NMR measurements.

^1H and ^1H – ^1H COSY (Correlation Spectroscopy) NMR measurements showed that in saturated DMSO solution the acidic forms existed, dimerisation took place, and there were hydrogen bonding

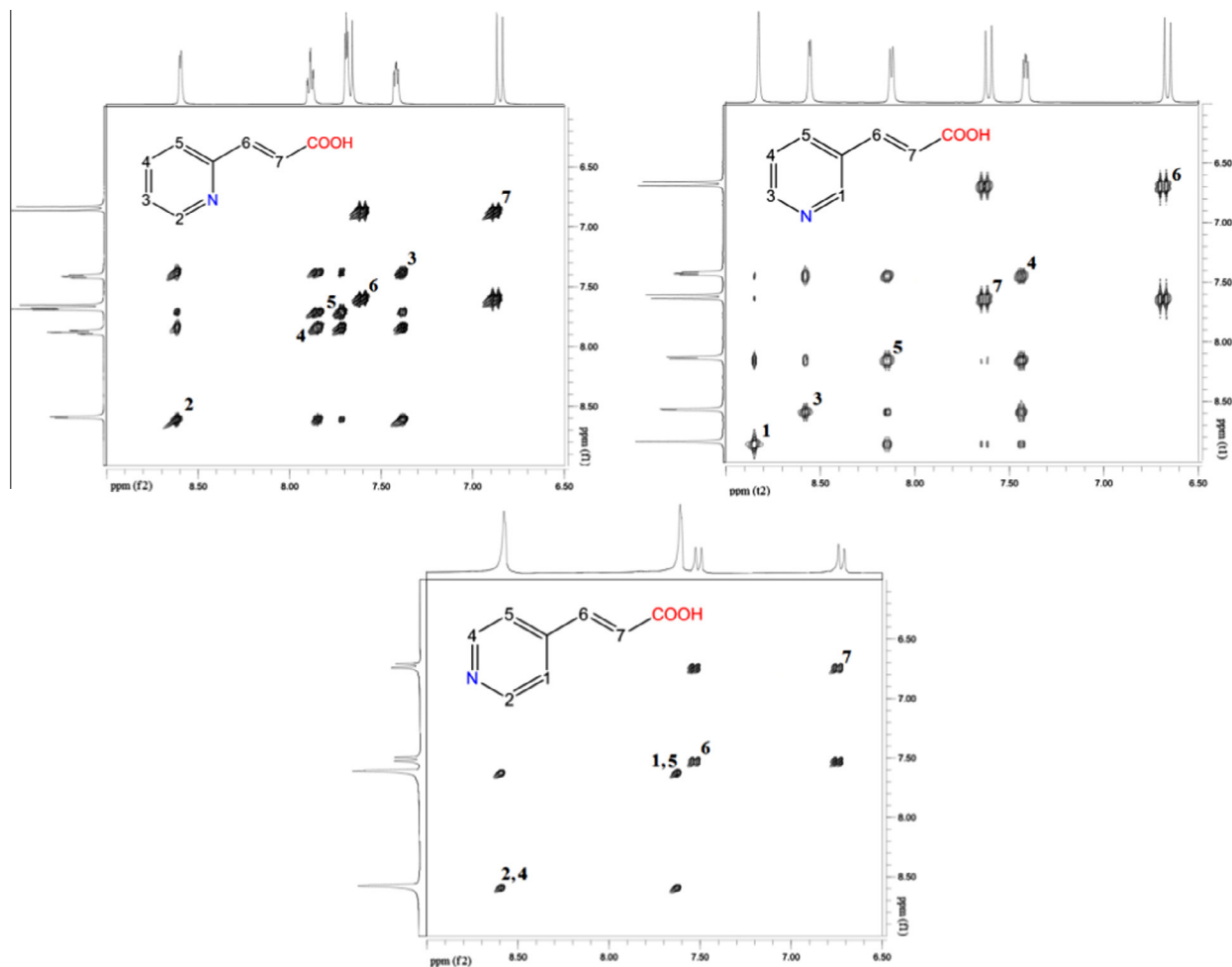
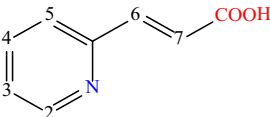
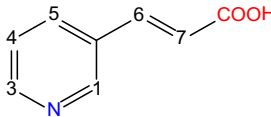
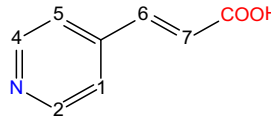


Fig. 4. ^1H – ^1H COSY NMR spectra of **E2P**, **E3P** and **E4P** molecules.

Table 1
Assignations of the ^1H NMR spectra in $\text{DMSO}-d_6$.

														
Proton	ppm	Splitting	Coupling	J (Hz)	ppm	Splitting	Coupling	J (Hz)		ppm	Splitting	Coupling	J (Hz)	
1	–	–	–	–	8.828	S	–	–		7.611	S	H1–H2	–	
2	8.590	D	H2–H3	3.9	–	–	–	–		8.577	S	H2–H1	–	
3	7.863	DD	H2–(H3)–H4	3.9 ; 5.7	8.557	D	H3–H4	4.1		–	–	–	–	
4	7.399	DD	H3–(H4)–H5	5.7 ; 4.9	7.414	DD	H3–(H4)–H5	4.1 ; 7.9		8.577	S	H4–H5	–	
5	7.687	D	H5–H4	5.7	8.123	D	H4–H5	7.9		7.611	S	H5–H4	–	
6	7.675	D	H6–H7	15.8	6.663	D	H6–H7	16.1		7.510	D	H6–H7	16.1	
7	6.844	D	H7–H6	15.8	7.609	D	H7–H6	16.1		6.725	D	H7–H6	16.1	
8	12.672	S	–	–	12.550	S	–	–		12.32	S	–	–	

interactions among the dimers (Fig. 4). The proton assignments for the three isomers are shown in Table 1 and inter- as well as intra-molecular couplings are listed in Tables 2 and 3. The coupling of protons next to the ring nitrogen to non-neighbouring protons indicates close contact between the rings of two molecules, in which the ring nitrogen is involved. This is a strong sign of $\text{C}=\text{H}\cdots\text{N}$ hydrogen bonding.

As shown in Table 2, several intermolecular (aromatic) $\text{C}=\text{H}\cdots\text{N}$ hydrogen bonds were detected in the correlation spectra, except the **E4P** isomer. Although the correlations were clearly seen, they did not show up as splittings in the 1D ^1H NMR spectra, since

the coupling constant among the non-neighbouring protons were too low to be observed under our detection conditions.

For the **E4P** isomer, no correlations could be identified in the spectrum, because the pyridyl ring has a C_2 symmetry (the pyridyl groups in both **E2P** and **E3P** have C_1 symmetry) resulting in two shifts and one strong spin–spin coupling masking the peaks relevant to the hydrogen bonds.

^1H – ^1H COSY spectra can provide information on the conformational behaviour as well, due to the possible long-range interactions between the aromatic and olefinic protons. Interaction, albeit a very weak one, was identified for each molecule, which

Table 2
Intermolecular couplings indicating intermolecular (aromatic) C–H...N hydrogen bonds.

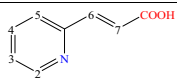
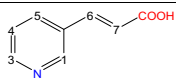
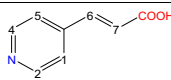
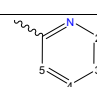
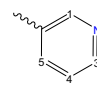
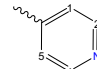
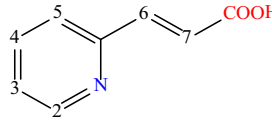
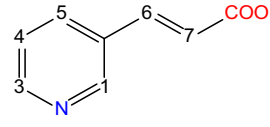
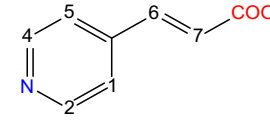
Molecules						
	Proton positions	2	1	3	2	4
	1	—	n/a	+	n/a	n/a
	2	n/a	—	—	n/a	n/a
	3	+	+	n/a	—	—
	4	+	+	n/a	n/a	n/a
	5	+	+	+	n/a	n/a

Table 3
Intramolecular couplings related to the conformational behaviour of the molecules.

Proton positions						
	6	7	6	7	6	7
1	–	–	n/a	–	n/a	n/a
5	n/a	n/a	n/a	–	n/a	n/a

means that the pyridyl group rotates almost freely in DMSO for **E2P**, **E4P** and **E3P** as well.

Choosing the methods for modelling hydrogen-bonded networks and conformational analysis

The results of the benchmarking calculations are shown in Tables 4 and 5. Table 4 shows the total time for the full geometry optimisation for the **E2P** monomer. As could be expected, the HF/

6-31G(d,p) method is the fastest, while the MP2/6-31G(d,p) method is the most time consuming. It is seen that taking into account Grimme's D3 dispersion scheme in the B3LYP calculations will not increase computational cost considerably, while using the CBSB7 basis set instead of smaller 6-31G(d,p) has a significant effect on the computational cost. Even so, the B3LYPD3/CBSB7 calculation takes less than one sixth of the time it takes to finish the MP2/6-31G(d,p) calculation. The CBS-4M method takes slightly less time to finish than the B3LYP/CBSB7 calculation, despite the high-level energy calculation it performs. This is likely due to the geometry optimisation phase, which is done at a relatively low level, and its importance will probably increase if the initial guess happens to be far from a stationary point.

Table 5 shows geometric parameters obtained for the **E2P** dimer with the different methods. The calculated (and corrected) bond energies are also shown. They were calculated with the following formula (Eq. (1)).

$$E_{\text{O-H}\cdots\text{O}} = E_{\text{dimer}} - (2E_{\text{monomer}}) \quad (1)$$

where $E_{\text{O-H}\cdots\text{O}}$ is the energy of the hydrogen bond between two molecules attached with double hydrogen bonds *via* the carboxylic groups, E_{dimer} is the (corrected) energy of the hydrogen bonded dimer, and E_{monomer} is the (corrected) energy of the monomer.

Table 4
Time (registered by the Gaussian package) needed for the geometry optimisation of the **E2P** monomer at various theoretical levels using the same hardware.

Method	CPU time (min)
B3LYP/6-31G(d,p)	24
B3LYP/6-31++G(d,p)	36
B3LYP/CBSB7	43
B3LYPD3/6-31G(d,p)	28
B3LYPD3/CBSB7	47
CBS-4M	37
HF/6-31G(d,p)	15
MP2/6-31G(d,p)	331

Table 5
Corrected (see, 'Computational methods') hydrogen bonding energies and the geometry parameters obtained at various theoretical levels for the hydrogen bonded dimer of **E2P** (1 He = 627.509 kcal/mol).

Method	E_{monomer} (He)	E_{dimer} (He)	O–H...O (kcal/mol)	H...O (pm)	O–H...O (°)
B3LYP/6-31G(d,p)	–514.284	–1028.581	–7.5	161	178.7
B3LYP/6-31++G(d,p)	–514.299	–1028.623	–15.6	162	179.5
B3LYP/CBSB7	–514.400	–1028.829	–18.9	165	179.8
B3LYPD3/6-31G(d,p)	–514.296	–1028.609	–10.3	160	178.9
B3LYPD3/CBSB7	–514.420	–1028.856	–8.8	164	179.7
CBS-4M	–511.371	–1022.746	–2.4	160	171.0
HF/6-31G(d,p)	–511.221	–1022.465	–13.4	180	176.3

The hydrogen bond energy of the O—H...O bonds in the dimer ranged from −2.4 kcal/mol for the CBS-4M method to the −18.9 kcal/mol of the B3LYP/CBSB7 method. The variation in the B3LYP calculations was notable, ranging from −7.5 kcal/mol to −18.9 kcal/mol. Each method resulted in completely planar geometry for the monomer and the dimer as well. Only small differences were found in the length of the double hydrogen bonds, and the decisive factor for choosing the method for further calculations was the energy of the hydrogen bond and the expense of the calculations. The choice was the B3LYP/6-31++G(d,p) method for the optimisation and energy calculation for the monomers and the agglomerates, since it provided reasonable hydrogen bonding energy values and geometric parameters (see, the values in ‘Computational methods’) at a reasonable computational cost. The HF/6-31G(d,p) method was applied for the conformational search of the monomers due to the lower computational cost comparing to other methods. This has importance, since the number of the calculations is several thousands.

Hydrogen bonding networks by modelling

As has been mentioned earlier, the dimer of the molecules can be chosen as the fundamental unit, at least in DMSO solution. The calculated energies for C=O...H—O hydrogen bonding and the bonding parameters for the three compounds are listed in Table 6, and the optimised geometries obtained at the B3LYP/6-31++G(d,p) level of theory are displayed in Fig. 5.

The aromatic C—H...N interaction between the neighbouring pyridyl rings, verified experimentally by the ¹H—¹H COSY spectra, are significantly weaker than the O—H...O hydrogen bonds keeping the dimers together, as it is revealed by the molecular modelling calculations at the B3LYP/6-31++G(d,p) level. An example for the optimised tetramer is displayed in Fig. 6, and the (corrected) hydrogen bond energies (calculated with Eq. (2)) and geometry parameters are listed in Table 7.

$$E_{\text{C—H...N}} = E_{\text{tetramer}} - (2E_{\text{dimer}}) \quad (2)$$

Table 6

Corrected (see, ‘Computational methods’) energy and geometry results for the acidic forms at the B3LYP/6-31++G(d,p) level.

Isomer	E_{monomer} (He)	E_{dimer} (He)	O—H...O (kcal/mol)	H...O (pm)	O—H...O (°)
E2P	−514.299	−1028.623	−15.6	162	179.5
E3P	−514.296	−1028.621	−17.5	163	179.6
E4P	−514.297	−1028.619	−15.4	162	179.6

Table 7

Corrected (see, ‘Computational methods’) energy and geometry results for the tetramers at the B3LYP/6-31++G(d,p) level.

Isomer	E_{dimer} (He)	E_{tetramer} (He)	C—H...N (kcal/mol)	H...N (pm)	C—H...N (°)
E2P	−1028.623	−2057.251	−3.1	257	149.3
E3P	−1028.621	−2057.246	−2.5	256	144.6
E4P	−1028.619	−2057.243	−2.9	250	145.3

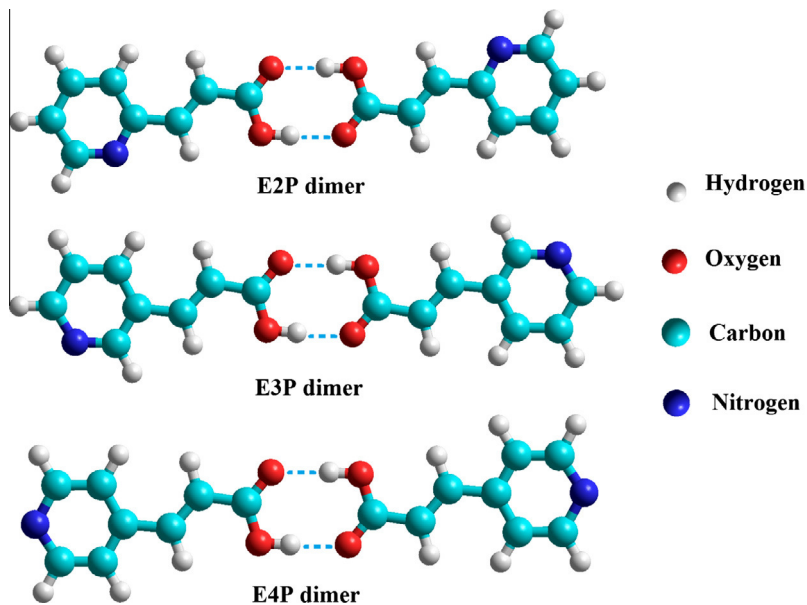


Fig. 5. Geometries of the dimers kept together via two C=O...O—H hydrogen bonds (represented with dashed blue lines) calculated at the B3LYP/6-31++G(d,p) level of theory. (For interpretation of the references to color in this figure legend, the reader is referred to the web version of this article.)

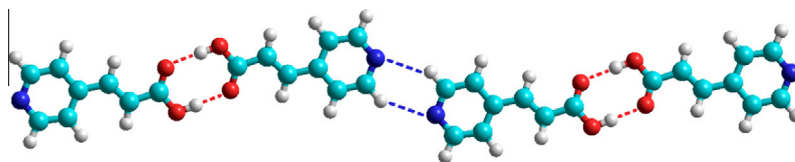


Fig. 6. The structure of the dimer of the dimers (tetramer) using the E4P molecule as an example, calculated at the B3LYP/6-31++G(d,p) level of theory.

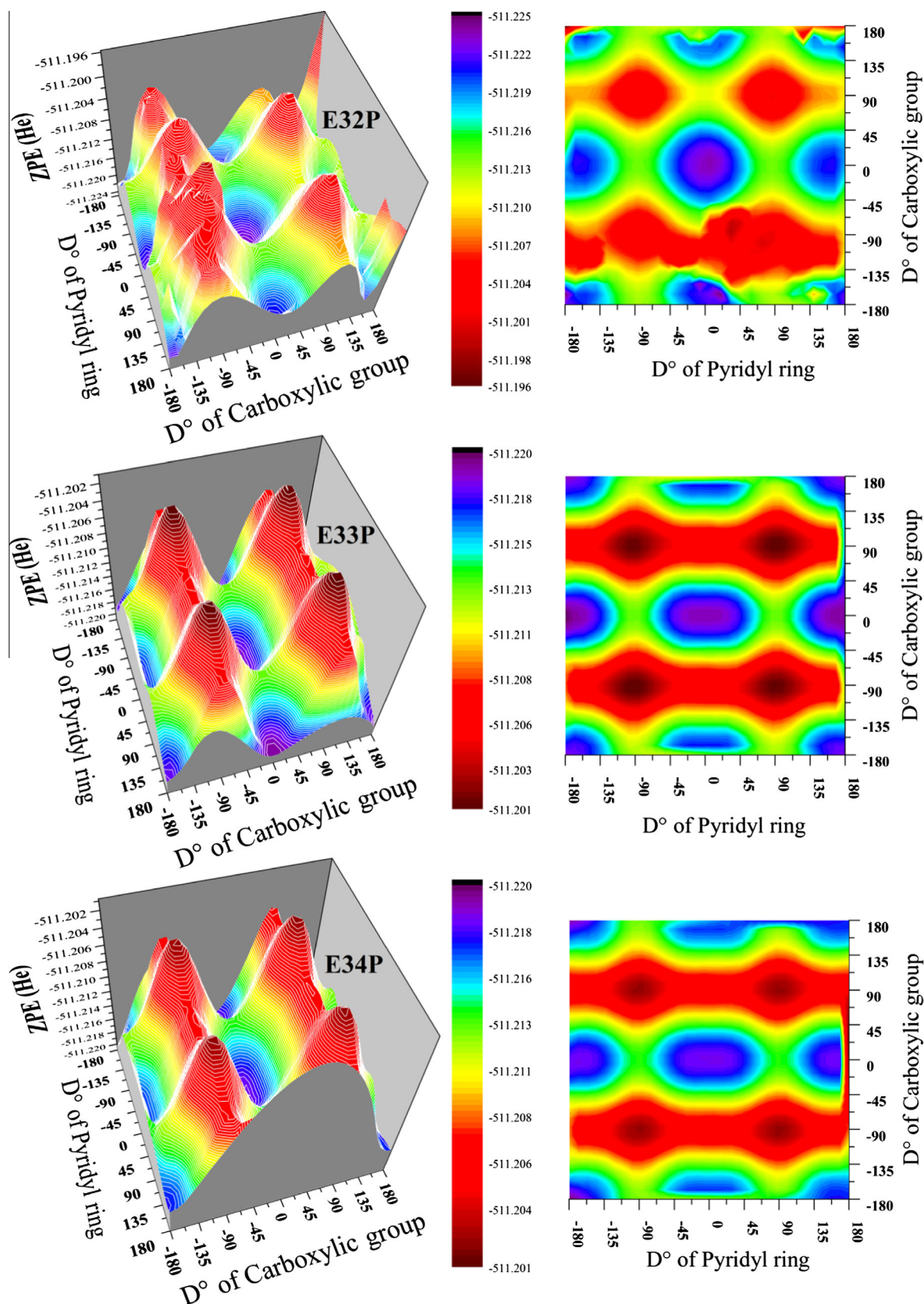


Fig. 7. The conformational energy surfaces and their cross sections of the molecules studied, calculated at the HF/6-31G(d,p) level of theory.

Conformational analysis

As it has already been described and explained, conformational analyses were performed at the HF/6-31G(d,p) level for the acidic

and for the zwitterionic forms (they have two torsions to be varied) to compare conformational behaviour. The conformational energy surfaces of the acidic monomers and the zwitterions (ZWs) are seen in Figs. 7 and 8.

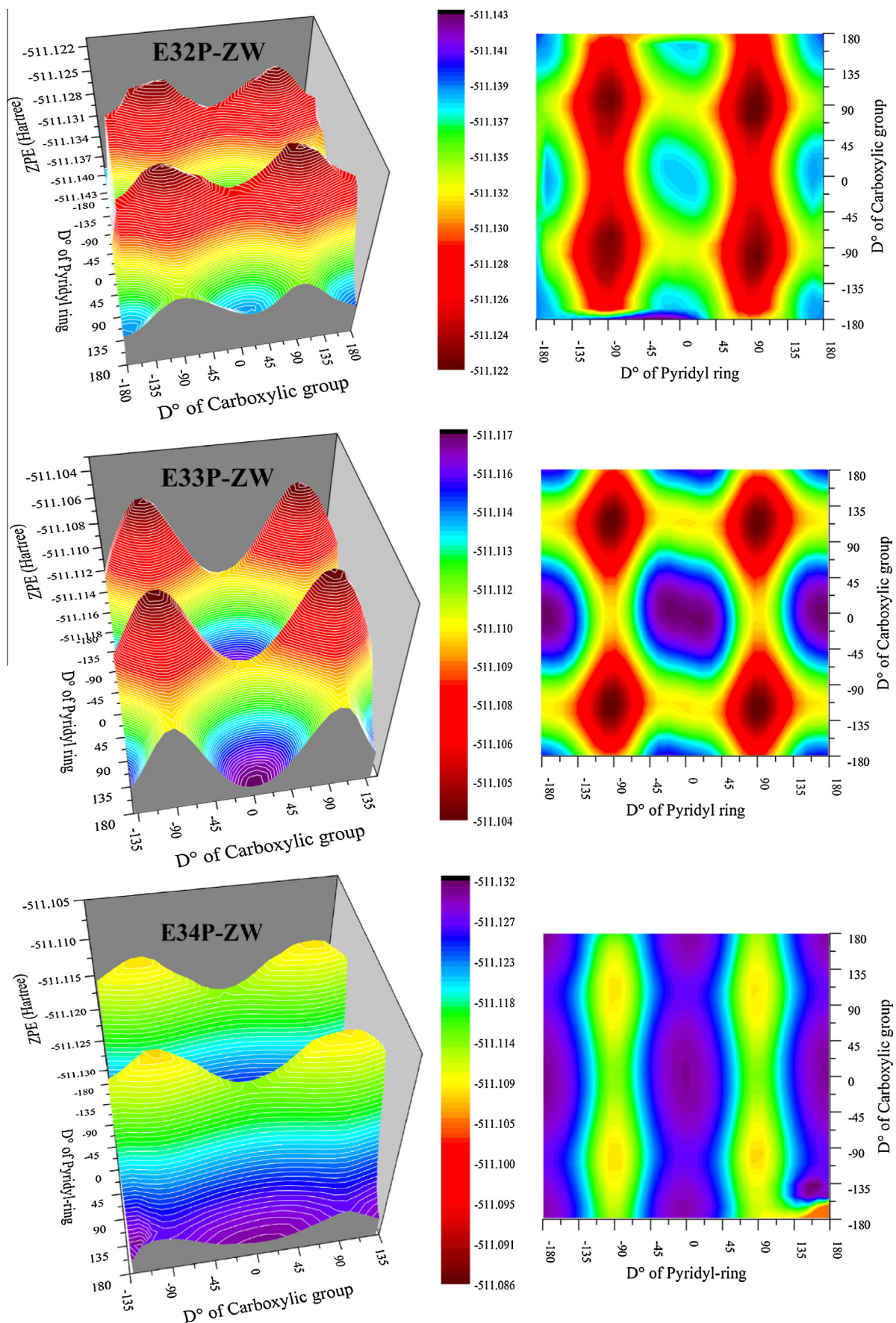


Fig. 8. The conformational energy surfaces and their cross sections of the zwitterionic structures studied, calculated at the HF/6-31G(d,p) level of theory.

If we count the structures that have smaller energy than 1 kcal/mol above the lowest found, it is clear that the zwitterion forms have slightly more stable conformers than the zwitterions (25 for **E2P**, 60 for **E3P**, 102 for the **E4P** and 70 for **E2P–ZW**, 94 for **E3P–ZW** and 104 for **E4P–ZW**); nevertheless, both structure-types are close to being planar (the dihedrals are close to being 0° and 0°). However, as indicated in Figs. 7 and 8, the pyridyl ring and the carboxylic group may flip by $\pm 180^\circ$, through lower saddle points. The **E2P** isomer has the highest rotational barrier (5.97–6.20 kcal/mol), possibly because of the plausible intramolecular C–H...N bond between the pyridyl nitrogen and the olefinic proton. The **E3P** and **E4P** isomers have lower barrier values (4.08 and 3.13 kcal/mol, respectively), which means that the interaction between the pyridyl ring and the other parts of the molecule is negligible. The results for the zwitterions are quite different due to their dipolar structure: rotational barriers are 3.43 kcal/mol, 4.29 kcal/mol and 10.87 kcal/mol, for the **E2P–ZW**, **E3P–ZW** and **E34P–ZW** structures, respectively.

Conclusions

The combination of instrumental methods and computations proved to be efficient for the description of the structure-forming properties of pyridylcinnamic acids, having the ring nitrogen in various positions. Instrumental methods indicated that zwitterionic species form the solid-state structure, while in the form of hydrochlorides acid dimers were the fundamental units. The acidic forms, found in DMSO, dimerise, and the dimers are kept together with strong C=O...HO carboxylic groups. The dimers were found to establish more extended aggregations via C–H...N hydrogen bonding. For these interactions, reasonable estimates for geometric as well as energy data could be derived after geometry optimisation performed at B3LYP/6-31++G(d,p) level of theory.

Acknowledgements

We thank the CSC–IT Center for Science Ltd. for computer time and technical assistance. The financial support by the TÁMOP-4.2.2.A-11/1/KONV-2012-0047 Grant, the Academy of Finland

(Centre of Excellence Program Project No. 1118615 and LASTU Program Project Number 135054), and ERC StG 257360-MOCAPAF is gratefully acknowledged.

References

- [1] I. Pálínkó, B. Török, M. Rózsa-Tarjányi, J.T. Kiss, Gy. Tasi, J. Mol. Struct. 348 (1995) 57–60.
- [2] I. Pálínkó, J.T. Kiss, Mikrochim. Acta [Suppl] 14 (1997) 253–255.
- [3] Á. Kukovecz, J.T. Kiss, I. Pálínkó, J. Mol. Struct. 408 (409) (1997) 325–327.
- [4] I. Pálínkó, Acta Crystallogr. B 55 (1999) 216–220.
- [5] Á. Kukovecz, I. Pálínkó, J. Mol. Struct. 482/483 (1999) 463–467.
- [6] J.T. Kiss, K. Felföldi, Z. Paksi, I. Pálínkó, J. Mol. Struct. 651 (2003) 253–258.
- [7] J.T. Kiss, K. Felföldi, I. Pálínkó, J. Mol. Struct. 744–747 (2005) 207–210.
- [8] B. Tolnai, J.T. Kiss, K. Felföldi, I. Pálínkó, J. Mol. Struct. 924–926 (2009) 27–31.
- [9] K. Csankó, L. Illyés, K. Felföldi, J.T. Kiss, P. Sipos, I. Pálínkó, J. Mol. Struct. 993 (2011) 259–263.
- [10] P. Brožič, B. Golob, N. Gomboc, T. Laňšník Rižner, S. Gobec, Mol. Cell. Endocrinol. 248 (2006) 233–235.
- [11] Y.-L. Chen, S.-T. Huang, F.-M. Sun, Y.-L. Chiang, C.-J. Chiang, C.-M. Tsai, C.-J. Weng, Eur. J. Pharm. Sci. 43 (2011) 188–194.
- [12] S. Fixon-Owoo, F. Levasseur, K. Williams, T.N. Sabado, M. Lowe, M. Klose, A.J. Mercier, P. Fields, J. Atkinson, Phytochemical 63 (2003) 315–334.
- [13] B. Narasimhan, D. Belsare, D. Pharande, V. Mourya, A. Dhake, Eur. J. Med. Chem. 39 (2004) 827–834.
- [14] I. Pálínkó, T. Körtvélyesi, Int. J. Quantum Chem. 84 (2001) 269–275.
- [15] B. Jójárt, I. Pálínkó, J. Mol. Model. 7 (2001) 408–412.
- [16] J. Csehi, I. Pálínkó, J. Mol. Model. 10 (2004) 151–154.
- [17] F. Freeman, L.Y. Chang, J.C. Kappos, L. Sumarta, J. Org. Chem. 52 (1987) 1460–1464.
- [18] B. Jovanovic, M. Misic-Vukovic, S. Drmanic, J. Csanádi, Heterocycles 37 (1994) 1495–1501.
- [19] E. Knoevenagel, Berichte 31 (1898) 2596–2619.
- [20] O. Doebner, Berichte 35 (1902) 1136–1137.
- [21] M.J. Frisch, G.W. Trucks, H.B. Schlegel, G.E. Scuseria, M.A. Robb, J.R. Cheeseman, G. Scalmani, V. Barone, B. Mennucci, G.A. Petersson, H. Nakatsuji, M. Caricato, X. Li, H.P. Hratchian, A.F. Izmaylov, J. Bloino, G. Zheng, J.L. Sonnenberg, M. Hada, M. Ehara, K. Toyota, R. Fukuda, J. Hasegawa, M. Ishida, T. Nakajima, Y. Honda, O. Kitao, H. Nakai, T. Vreven, J.A. Montgomery Jr., J.E. Peralta, F. Ogliaro, M. Bearpark, J.J. Heyd, E. Brothers, K.N. Kudin, V.N. Staroverov, R. Kobayashi, J. Normand, K. Raghavachari, A. Rendell, J.C. Burant, S.S. Iyengar, J. Tomasi, M. Cossi, N. Rega, J.M. Millam, M. Klene, J.E. Knox, J.B. Cross, V. Bakken, C. Adamo, J. Jaramillo, R. Gomperts, R.E. Stratmann, O. Yazyev, A.J. Austin, R. Cammi, C. Pomelli, J.W. Ochterski, R.L. Martin, K. Morokuma, V.G. Zakrzewski, G.A. Voth, P. Salvador, J.J. Dannenberg, S. Dapprich, A.D. Daniels, Ö. Farkas, J.B. Foresman, J.V. Ortiz, J. Cioslowski, D.J. Fox, Gaussian 09, Revision D.01, Gaussian, Inc., Wallingford CT, 2009.
- [22] S.F. Boys, F. Bernardi, Mol. Phys. 19 (1970) 553–566.
- [23] S. Simon, M. Duran, J. Dannenberg, J. Chem. Phys. 105 (1996) 11024–11031.
- [24] A. Winkler, J.B. Mehl, P. Hess, J. Chem. Phys. 100 (1994) 2717–2727.